Toxicology Reports 2 (2015) 838–849

Contents lists available at ScienceDirect

Toxicology Reports

journal homepage: www.elsevier.com/locate/toxrep

The use of urinary and kidney SILAM proteomics to monitor kidney response to high dose morpholino oligonucleotides in the mdx mouse

Aiping Zhang, Kitipong Uaesoontrachoon, Conner Shaughnessy, Jharna R. Das, Sree Rayavarapu, Kristy J. Brown, Patricio E. Ray, Kanneboyina Nagaraju, John N. van den Anker, Eric P. Hoffman, Yetrib Hathout*

The Centers for Genetic Medicine Research and Translational Science, Children's Research Institute, Children's National Medical Center, 111 Michigan Avenue, NW, Washington, DC 20010, USA

ARTICLE INFO

Article history:
Received 11 February 2015
Received in revised form 7 May 2015
Accepted 7 May 2015
Available online 19 May 2015

Chemical compounds studied in this article:
Phosphorodiamidate morpholino (PubChem CID: 22140692)
Isoflurane (PubChem CID: 3763)
Formic acid (PubChem CID: 284)
Acetonitrile (PubChem CID: 6342)
Acetone (PubChem CID: 180)
Methanol (PubChem CID: 887)

Keywords:
PMO
Urinary biomarkers
mdx-23
Duchenne muscular dystrophy
Clusterin
GGT1

ABSTRACT

Phosphorodiamidate morpholino oligonucleotides (PMO) are used as a promising exon-skipping gene therapy for Duchenne muscular dystrophy (DMD). One potential complication of high dose PMO therapy is its transient accumulation in the kidneys. Therefore new urinary biomarkers are needed to monitor this treatment. Here, we carried out a pilot proteomic profiling study using stable isotope labeling in mammals (SILAM) strategy to identify new biomarkers to monitor the effect of PMO on the kidneys of the dystrophin deficient mouse model for DMD (mdx-23). We first assessed the baseline renal status of the mdx-23 mouse compared to the wild type (C57BL10) mouse, and then followed the renal outcome of mdx-23 mouse treated with a single high dose intravenous PMO injection (800 mg/kg). Surprisingly, untreated mdx-23 mice showed evidence of renal injury at baseline, which was manifested by albuminuria, increased urine output, and changes in established urinary biomarker of acute kidney injury (AKI). The PMO treatment induced further transient renal injury, which peaked at 7 days, and returned to almost the baseline status at 30 days post-treatment. In the kidney, the SILAM approach followed by western blot validation identified changes in Meprin A subunit alpha at day 2, then returned to normal levels at days 7 and 30 after PMO injection. In the urine, SILAM approach identified an increase in Clusterin and γ-glutamyl transpeptidase 1 as potential candidates to monitor the transient renal accumulation of PMO. These results, which were confirmed by Western blots or ELISA, demonstrate the value of the SILAM approach to identify new candidate biomarkers of renal injury in mdx-23 mice treated with high dose PMO.

Abbreviations: 5-OPase, 5-oxoprolinase; Aass, alpha-aminoadipic semialdehyde synthase; AKI, acute kidney injury; AMY2, pancreatic amylase α2; Anx2, annexin 2; AP-A, glutamyl aminopeptidase; AP-N, aminopeptidase N; CI-B22, NADH dehydrogenase [ubiquinone] 1 beta subcomplex subunit 9; Cytcox, cytochrome c oxidase subunit 2; DMD, Duchenne muscular dystrophy; EGF, pro-epidermal growth factor; FABPH, fatty acid binding protein heart type; PK, pharmacokinetics; GGT1, gamma glutamyltransferase 1; H&E, hematoxylin and eosin; IP2, integrated proteomics pipeline; KIM-1, kidney injury molecule-1; mAspAT, mitochondrial aspartate aminotransferase; Mep-1, Meprin A subunit alpha; NGAL, neutrophil gelatinase-associated lipocalin; OPN, osteopontin; PAS, periodic acid shift; PCB, mitochondrial pyruvate carboxylase; PMO, phosphorodiamidate morpholino oligonucleotide; PSs, phosphorothioates; SILAM, stable isotope labeling in mammals; SUn, serum urea nitrogen.

* Corresponding author at: The Center for Genetic Medicine Research, Children's National Medical Center, 111 Michigan Avenue, NW, Washington, DC 20010, USA. Tel.: +1 202 476 3136; fax: +1 202 476 6014.

E-mail addresses: azhang@childrensnational.org (A. Zhang), kitiponguaesoontrachoon@gmail.com (K. Uaesoontrachoon), cshaughnessyo@gmail.com (C. Shaughnessy), JDas@childrensnational.org (J.R. Das), drrayavarapu@gmail.com (S. Rayavarapu), kristy.brown@childrensnational.org (K.J. Brown), PRAY@childrensnational.org (P.E. Ray), KNagaraju@childrensnational.org (K. Nagaraju), JVandena@childrensnational.org (J.N. van den Anker), EHoffman@childrensnational.org (E.P. Hoffman), YHathout@childrensnational.org (Y. Hathout).

http://dx.doi.org/10.1016/j.toxrep.2015.05.008

1. Introduction

Therapeutic oligonucleotides have received sustained interest due to the high specificity to their mRNA or microRNA targets, and effectiveness in inhibiting their target [1,2]. Multiple chemistries are under development with goals of optimizing cellular delivery, affinity and specificity for the target. As with most drugs, toxicity findings may limit the doses of the oligonucleotides that can be safely administered. Acute inflammatory reactions can be a dose-limiting toxicity, but are observed with some chemistries such as phosphorothioates (PSs) [3–5], but not others such as phosphorodiamidate morpholino oligonucleotides (PMO) [6]. Target organs for oligonucleotide drugs typically include the liver and kidney, where these drugs accumulate causing cellular toxicity prior to being metabolized and/or excreted by these tissues [7–9].

The large majority of oligonucleotide drugs utilize a PSs chemical linkage between adjacent nucleotides. This linkage has been shown to improve stability by reducing cleavage by nucleases. PSs drugs also show strong pharmacokinetic and pharmacodynamic profiles [10]. However, PSs drugs may also show off-target protein binding and induction of complement or other inflammatory pathways. The PMO chemistry seems entirely resistant to nuclease cleavage, and shows no induction of inflammatory pathways at very high doses [6,11,12].

Clinical development of PMO chemistry is most advanced in applications to exon-skipping in Duchenne muscular dystrophy (DMD) [13–15]. DMD is caused by dystrophin deficiency in myofibers, leading to plasma membrane instability. Overt breaches of the dystrophin-deficient myofiber membranes appear to provide a delivery route for the PMO drugs, thus bypassing the otherwise rapid clearance [16,17]. Pre-clinical studies conducted in murine and canine models for DMD showed that systemic IV injection of PMO drug successfully restored the missing dystrophin protein in skeletal muscle with concomitant improved functional outcomes [18–21]. Both biochemical and clinical efficacy is dose responsive, with high doses (100–300 mg/kg/wk.) showing the most pronounced long-term therapeutic effects, a finding likely related to the presumed bulk flow process of drug delivery across unstable myofiber membranes.

Previous toxicity studies performed on the dystrophin deficient mouse model for DMD (mdx-23) and monkeys [12], showed that weekly injections of high doses of PMO (960 mg/kg/wk in mice; 320 mg/kg/wk in monkeys), can induce transient renal tubular injury. PMO is accumulated in renal proximal tubular cells, in a similar manner to other oligonucleotide drugs [6]. From the renal histological view, the accumulation of PMO in renal tubules is associated with flattened tubular epithelium, basophilic granules, and mild tubular vacuolation [6,12]. These lesions, however, are considered dose-dependent and potentially reversible [12]. Therefore, because PMO appears a promising treatment for patients with DMD, it is necessary to further evaluate the effect of PMO on kidneys and identify new urine biomarkers to monitor the renal PMO load and outcome for DMD patients [22].

Urine is a readily accessible body fluid and useful source for biomarker discovery and assessment of the renal effects of cytotoxic drugs [23–27]. Here, we carried out a pilot proteome profiling study to follow the renal outcome of the mdx-23 mouse after a single intravenous injection of high dose PMO (800 mg/kg). More specifically, we analyzed kidney and urine proteomes collected from PMO and saline treated mdx-23 mice using SILAM strategy in combination with high precision LC–MS/MS analysis of peptides, and bioinformatics mapping to parent proteins (supplemental Fig. S4). Subsequently, we verified the positive findings by Western blots or ELISA assay using all mouse groups. This approach identified an alterations in the levels Meprin A subunit alpha (Mep-1) in the kidney and an increase of two urine accessible candidate biomarkers clusterin, and gamma glutamytransferase 1 (GGT1) (Fig. 1), that may become a useful biomarker profile to monitor the renal outcome of patients treated with PMO and other oligonucleotides.

2. Material and methods

2.1. Animal experiments

All experiments were reviewed and approved by the Institutional Animal Care and Use Committee (IACUC) of Children's National Medical Center (protocol # 199-01-07 for ^{15}N labeled SILAM [Stable isotope labeling by amino acids in mouse]; protocol # 304-13-04 for toxicity test of PMO oligonucleotide therapy).

The animal models used in this study included the mdx-23 mouse model having a spontaneous *DMD* gene mutation causing a splice site mutation in exon 23 on the C57BL/10 background (C57BL/10ScSn-Dmdmdx/J). Wild-type background strain (C57BL/10) was used as baseline control. All mice were purchased from Jackson Laboratory, Bar Harbor, Maine.

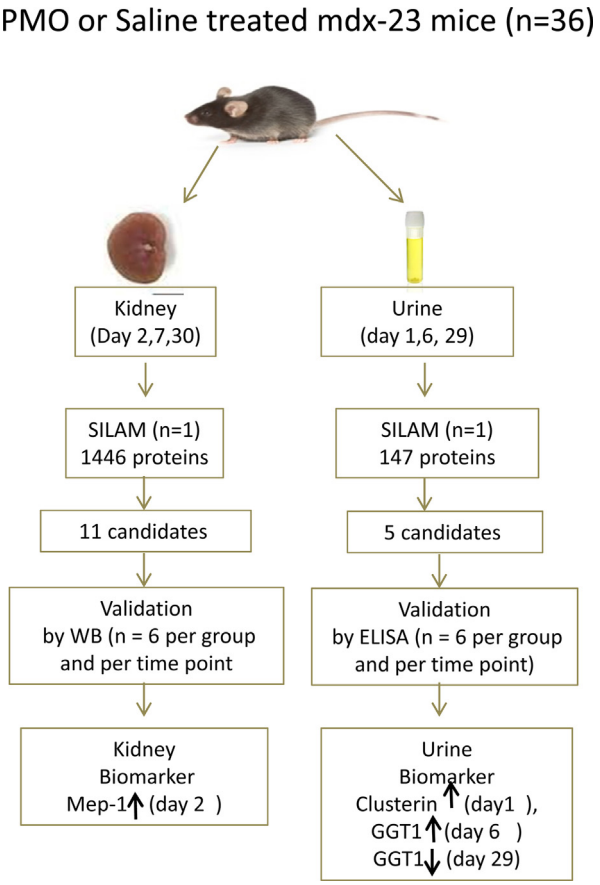

Fig. 1. Overall study design. Mdx23 (n = 36) randomly divided two groups, one group (n = 18) was treated with a single high dose (800 mg/kg) and the second group (n = 18) was treated with the same volume of saline vehicle. Urine samples at days 1, 6, and 29 urine while kidneys were collected at days 2, 7 and 30 following treatment (n = 6 per group and per time point). For SILAM proteome profiling of urine and kidney samples one mouse was randomly selected from PMO and saline treated group and at each time point totaling 6 urine samples and 6 kidney samples for LC–MS/MS analysis. Protein that were found differentially altered in kidney and urine samples were further validated by western blotting for kidney extract and ELISA for urine samples (samples size n = 6 per group per time point); also urine candidates validated by ELISA (samples size n = 6 per group per time point). Mep-1 increased day 2 as a, potential biomarker in kidney and clusterin increased day 1 and GGT1 increased day 6, decreased at day 29 as potential urinary biomarkers which associated with PMO kidney loading and clearance.

2.2. ^{15}N labeled mouse

A previously reported stable isotope labeling in mammals (SILAM) strategy was used to generate a stock of ^{15}N-labeled tissue and body fluids proteome atlases as an internal standard for accurate proteome profiling experiments [28,29]. Briefly, 3 week old C57BL6 male were fed a chow of ^{15}N enriched Spirulina (MouseExpress, $^{15}N = 98\%$; Cambridge Isotope Laboratories, Andover, MA). Labeling efficiency of urine proteins was monitored weekly using mass spectrometry analysis and Integrated Proteomics Pipeline tool (IP2 version 1.42). Sufficient urinary proteome labeling with ^{15}N was defined as >95% of peptides showing full labeling with the heavy isotope ^{15}N, and this level was reached by 12 weeks of feeding ^{15}N enriched Spirulina (supplemental Fig. S2). Both ^{15}N labeled urine protein and ^{15}N-labeled kidney proteins were used as internal to profile protein in urine and kidneys of PMO treated and untreated mdx-23 mice as described below.

2.3. Study design

Seven-week-old mdx-23 male mice ($n = 36$) were randomly divided into two groups and each mouse was ear tagged with specific ID number for follow up studies. Each mouse in the PMO treated group ($n = 18$) was injected with a single high dose PMO (800 mg/kg dissolved in 200 μL saline solution, AVI-4225, GGC CAA ACC TCG GCT TAC CTG AAA T) via a retro-orbital vein while the control group ($n = 18$) was injected with 200 μL saline vehicle. Baseline urine samples were collected from each mdx-23 mouse before treatment with PMO or saline solution then at 30 min, 45 min, 60 min, 90 min, 120 min, 180 min and 360 min post-treatment. These urine samples were used for PMO urinary PK. Further urine samples were collected for a period of 4 h at days 1, 6, 14, 20 and 29 post-treatment, and randomly selected one mouse sample at days 1, 6 and 29 just before sacrificed mice from each group used for proteome profiling. All urine samples ($n = 6$ per group and per time point) used for further validation by ELISA assays. Then six mice per group and per time point were sacrificed at days 2, 7 and 30 to collect kidneys for histology and proteome profiling. At each time point mice were anesthetized using isoflurane and blood was collected via cardiac puncture before kidneys were removed, and serum samples prepared and stored at −80 °C for later analyses (Fig. 1). Each kidney was cut longitudinally into two halves, one half was snap-frozen in liquid nitrogen-cooled isopentane and stored at −80 °C for later molecular analyses while the other half was fixed in 10% neutral formalin solution for histopathological analyses.

Additional urine samples were collected from mdx23 mice and age matched wild type C57BL/10 male mice ($n = 12$ per group) for baseline urine AKI ELISA assay (Table 1).

Urine collection was done using a previously described method [30] with minor changes. Briefly, individual mouse was placed in clean cages without bedding, food or water for 4 h. Urine droplets in the bottom of the cage were recovered, and transferred to small tubes and chilled. Average urine volume collected from each mouse ranged from 100 μL to 500 μL. The collected urine samples were centrifuged at 14,000 × *g* for 5 min at 4 °C. Supernatants were collected and stored in small volume aliquots (10 μL) at −80 °C for later analyses.

2.4. Measurement of PMO excretion

To measure urinary excretion of PMO we used a mass spectrometry approach for analysis of 10 μL urine aliquots collect at 0, 30 min, 45 min, 60 min, 90 min, 120 min, 180 min, and 360 min following injection of mdx-23 mice with single high dose PMO (800 mg/kg). Proteins were precipitated by addition of 200 μl methanol, followed by 1 h incubation at room temperature. Samples were then centrifuged for 10 min at 14,000 × *g* and supernatants containing the PMO were saved. The pellet was washed with 100 μl of 100 mM Tris, pH 7, then centrifuged again and supernatants pooled. Supernatants containing PMO were dried by vacuum centrifugation in Reacti-vials then resuspended in 50 μl of water, heated for 5 min at 60 °C and allowed to cool to room temperature. The sample was then processed using BioRad BioSpin 6 columns and Millipore C18 ZipTips using manufacturer's instructions. The ZipTip eluent was analyzed by static nanospray on a Thermo OrbitrapXL at 100,000 resolution and 800–2000 *m*/*z*. Spectra were deconvoluted using Thermo Xtract software. Signal intensities of injected morpholino were plotted vs. time.

2.5. Measurement of urine creatinine, protein concentration and serum urea nitrogen

Urine creatinine levels were measured using Creatinine Assay Kit (R&D Systems, Minneapolis, MN) based on the Jaffe alkaline picrate method and following the manufacturer recommended protocol. Serum urea nitrogen (SUn) was determined using QuantiChrom™ Urea Assay Kit (BioAssay System, Atlanta, GA) following the manufacturer recommended protocol. To measure protein concentration in collected urine samples, pre-cooled 40 μl distilled and deionized water (ddH_2O) and 200 μl of pre-chilled acetone (overnight at −20 °C) were added to 10 μL urine. The sample was vigorously mixed and incubated at −20 °C for 30 min, then centrifuged at 14,000 × *g* 4 °C, for 15 min. Precipitated proteins were resuspended in 40 μl ddH_2O and protein content was measured using Pierce BCA assay (Thermo Scientific, Rockford, IL). Protein excretion calculation formula: protein concentration × volume/minutes (4 h); urine output calculation formula: total urine volume/minutes (4 h).

2.6. Renal histopathology

Formalin-fixed kidneys ($n = 6$ per group and per time point) were paraffin-embedded, and 4 micron sagittal sections cut and stained with hematoxylin and eosin (H&E) or Periodic Acid Shift (PAS) as previously described [31]. All slides were given a renal cortical tubular injury score using a semi-quantitative scale [32–34]. Because of the exploratory nature of the study and the small sample size, evaluation of kidney histology was performed in non-blinded fashion. Ten microscopic fields were examined in each section under 20× and 40× magnifications for histological evidence

Table 1A
Baseline urine flow rate and analysis in wild type C57BL10 and mdx23 mice (mean ± SD).

Strain	Age (weeks)	Timed urine collection (min)	Urine protein (μg/μl)	Urine creatinine (mg/dl)	protein Excretion (μg/min)	Urine output (μl/min)
C57BL10 ($n = 12$)	7	240	4.16 ± 1.44	37.07 ± 5.98	15.35 ± 2.40	3.33 ± 1.23
mdx23 ($n = 12$)	7	240	5.68 ± 1.04	21.92 ± 2.55	34.13 ± 9.17	6.50 ± 1.76
Folds (mdx23/C57BL10)			1.37	0.59	2.25	1.95
P value			0.0466	<0.0001	<0.0001	<0.0001

$P < 0.05$ is significant.

Table 1B
Base line comparison of AKI urinary biomarkers in mdx23 and wild type C57BL10 mice (mean ± SD).

Strain	Albumin (μg/ml)	KIM1 (pg/ml)	Cystatin C (μg/ml)	Clusterin (μg/ml)	EGF (μg/ml)	NGAL (ng/ml)	GGT1 (ng/ml)	OPN (μg/ml)
C57BL10 (n = 12)	36.34 ± 9.74	74.45 ± 2.86	0.10 ± 0.02	0.84 ± 0.27	0.81 ± 0.20	1.23 ± 0.58	11.30 ± 0.91	1.22 ± 0.33
mdx23 (n = 12)	75.97 ± 21.52	72.44 ± 4.99	0.13 ± 0.03	0.72 ± 0.17	0.48 ± 0.03	4.21 ± 0.73	11.69 ± 3.67	1.06 ± 0.29
Folds (mdx23/C57BL10)	2.09	0.97	1.3	0.86	0.51	3.42	1.03	0.87
P value	<0.0001	>0.05	0.0175	>0.05	<0.001	<0.0001	>0.05	>0.05

Abbreviations: AKI, acute kidney injury; KIM1, kidney injury molecule-1; EGF, pro-epidermal growth factor; NGAL, neutrophil gelatinase-associated lipocalin; GGT1, gamma-glutamyltranspeptidase 1; OPN, osteopontin. P values < 0.05 are significant.

of tubular injury, which included single or multiple tubular cells undergoing necrosis (defined as nuclear condensation, cytoplasmic swelling, and focal loss of nuclei), tubular dilatation, microcysts, proteinaceous cast, and recruitment of inflammatory cells. The percentage of the renal cortical area exhibiting any of these lesions were scored as followed: 0 = normal kidney, 1 = minimal tubular injury < 5% involvement; 2 = mild tubular injury (6–20% involvement); 3 = moderate tubular injury (21–50% involvement); and 4 = severe tubular injury (>50% involvement).

2.7. Proteomic profiling

Urine samples (15 μL) from PMO and saline treated mice (n = 1 per group and per time point) were each spiked with 7.5 μL of ^{15}N labeled urine sample collected from ^{15}N-labeled SILAM mouse. Mixed samples were fractionated by SDS-PAGE using 4–12% NuPAGE® Novex® Bis-Tris gels. Gels were stained with Bio-Safe Coomassie blue (Bio-Rad, Hercules, CA), and each sample lane cut into 23–24 serial slices. Each gel slice was then in-gel digested with trypsin (10–20 μl 12.5 ng/μl in 50 mM NH_4HCO_3) (Promega, Madison, WI), and the resulting peptides were extracted and analyzed by LC–MS/MS as described below.

Kidney tissue protein extraction and analysis was done by homogenization and lysis of the frozen samples in without detergent lysis buffer (1 mM potassium phosphate monobasic, 3 mM sodium phosphate dibasic, 155 mM NaCl, Roche protease inhibitor cocktail tablets, pH 7.4) using a motor-driven Potter-Elvehjem homogenizer and sonication (Polytron, 3 × 30 s bursts). Protein concentration was determined in each sample using BCA assay (Thermo scientific, Rockford, IL). Each kidney protein extract (50 μg aliquot) was spiked with 25 μg of ^{15}N labeled kidney protein extract prepared from a SILAM mouse. Spiked samples were then further fractionated by SDS-PAGE as described above and processed for in gel digestion similarly as urine samples.

Peptide mixtures from each gel band were resuspended in 10 μL of 0.1% formic acid and loaded (6 μL) via an auto-sampler onto a Symmetry C18 trap column (5 μm, 300 μm inner diameter × 23 mm, Waters Milford, MA). The trapped peptides were washed for 10 min with 0.1% formic acid at a flow rate of 10 μL/min then eluted on a C18 reversed-phase column (3.5 μm, 75 μm × 15 cm, LC Packings Sunnyvale, CA) at a flow rate of 250 nL/min using a Nano-HPLC system from Eksigent (Dublin, CA) and a mobile phase consisting of water with 0.1% formic acid (A) and 90% acetonitrile (B). A 65-min linear gradient from 5% to 40% B was employed. Eluted peptides were introduced into the mass spectrometer via a 10 μm silica tip (New Objective Inc., Ringoes, NJ) adapted to a nano-electrospray source (Thermo Fisher Scientific). The spray voltage was set at 1.2 kV, and the capillary heated to 200 °C. The LTQ-Orbitrap-XL (Thermo Fisher Scientific) was operated in data-dependent mode with dynamic exclusion, in which one cycle of experiments consisted of a full MS survey scan in the Orbitrap (300–2000 m/z, at 30,000 resolution) and five subsequent MS/MS scans in the LTQ of the most intense peaks, using collision-induced dissociation with helium gas and normalized collision energy value set at 35%.

2.8. Database search and SILAM ratio measurement

For protein identification and quantification we used Integrated Proteomics Pipeline (IP2) version 1.42 software developed by Integrated Proteomics Applications, Inc. (http://www.integratedproteomics.com/). IP2 uses the Sequest search engine version 2010 (06 10 13 1836). Each raw MS and MS/MS file was searched against the forward and reverse UniProt mouse database (UniProt release 15.15, January 2013, 16,580 forward entries) tryptic peptides allowing two missed cleavages and the possible modifications of Met residue by oxidation (+15.99492 Da) and nitrogen atoms (+0.98 Da) to account for ^{15}N labeled peptides. Because of the wide isotope distribution of ^{15}N labeled peptides the mass tolerance was set at ±300 ppm (15 N) for MS and ±1.5 Da for MS/MS. Data were filtered by setting the protein false discovery rate (FDR) at 1%. Only proteins that were identified by at least two unique peptides were retained for further quantitative analysis. Census software (version 1.77), built into the IP2 platform, was used to determine the ratios of light to heavy peptide pairs using an extracted chromatogram approach. Quantitative data were filtered based on a determinant value of 0.5 and an outlier P-value of 0.1.

2.9. ELISA assays

Mouse specific osteopontin (OPN), pro-epidermal growth factor (EGF), neutrophil gelatinase-associated lipocalin (NGAL), Kidney Injury Molecule-1 (KIM-1), Cystatin C and clusterin ELISA assay kits were purchased from R&D Systems, Inc. (Minneapolis, MN); albumin ELISA kit was from Bethy Laboratories, Inc. (Montgomery, TX); and pancreatic amylase α2 (AMY2) and γ glutamytransferase 1 (GGT-1) kits were from BlueGene, Biotech (Putuo District, Shanghai). Urine aliquots (10 μL) from each PMO and saline treated mouse at each time point were used in duplicate in each assay following the manufacturer's recommended protocols.

Table 1C
Creatinine normalization of base line comparison of AKI urinary biomarkers in mdx23 and wild type C57BL10 mice (mean ± SD).

Strain	Albumin (μg/mg)	KIM1 (ng/mg)	Cystatin C (μg/mg)	Clusterin (μg/mg)	EGF (μg/mg)	NGAL (ng/mg)	GGT1 (ng/mg)	OPN (μg/ml)
C57BL10 (n = 12)	98.19 ± 21.50	0.20 ± 0.03	0.28 ± 0.04	2.26 ± 0.63	2.17 ± 0.37	69.21 ± 31.31	31.20 ± 14.97	3.29 ± 0.71
mdx23 (n = 12)	384.22 ± 98.85	0.33 ± 0.03	0.60 ± 0.05	3.30 ± 0.64	2.17 ± 0.32	384.0 ± 58.05	53.82 ± 19.60	4.81 ± 1.01
Folds (mdx23/C57BL10)	3.91	1.65	2.14	1.46	1	5.55	1.72	1.46
P value	<0.0001	<0.0001	<0.0001	0.0006	>0.05	<0.0001	0.0044	0.0003

Abbreviations: AKI, acute kidney injury; KIM1, kidney injury molecule-1; EGF, pro-epidermal growth factor; NGAL, neutrophil gelatinase-associated lipocalin; GGT1, gamma-glutamyltranspeptidase 1; OPN, osteopontin. P values < 0.05 are significant.

2.10. Western blot analysis

Kidney protein-extracts (20 μg aliquots) were fractionated by SDS-PAGE on 4–12% NuPAGE® Novex® Bis-Tris gels (Invitrogen, Grand Island, NY). Separated proteins were transferred to nitrocellulose membranes (Millipore, Billerica, MA, USA) at 300 mA for 90 min at room temperature. Membranes were blocked in TBS-T (20 mM Tris pH 7.5, 500 mM NaCl, 0.1% Tween 20) supplemented with 5% non-fat dry milk (Bio-Rad) for 1 h at room temperature. Blots were probed with the following primary antibodies: goat anti-Aminopeptidase N (AP-N), goat anti-Meprin A subunit alpha (Mep-1) and rabbit anti-glutamyl aminopeptidase (AP-A) (R&D system, 1:1000), rabbit anti-fatty acid binding protein heart type (FABPH) (1:200, Gene Tax), rabbit anti-11-fold increase in NADH dehydrogenase [ubiquinone] 1 beta sub complex subunit 9 (CI-B22) (1:500, Gene Tax) and mouse anti-vinculin (1:2000, Cell Signaling) with the corresponding horseradish peroxidase-conjugated secondary antibody (1:5000–1:20,000 dilution). Blots were processed using an ECL detection kit (GE Life, Pittsburgh, PA) and exposed to X-ray films. For quantification, films were scanned using a Bio-Rad GS-800 calibrated densitometer running Quantity One software (Bio-Rad). Optical density of each specific band was analyzed using Image J Software.

2.11. Statistical analyses

Unpaired two-tailed Student's *T* test was used for simple two group assessments. Differences between mean value of PMO and saline groups, or among different time points were considered significant when the $P < 0.05$.

3. Results

3.1. Dystrophin deficient mdx-23 mice develop spontaneous renal injury and show changes in urinary biomarkers of AKI

Prior to determining the effects of high dose PMO on the kidneys of the mdx-23 mouse model for DMD, we assessed the baseline renal status of these mice in comparison with age matched C57BL10 wild type control mice. Surprisingly, we found that 7 week old male mdx-23 mice develop significant proteinuria (2.25 fold increase over wild-type; $P < 0.0001$), and increased urine output (1.95 fold, $P < 0.0001$) when compared to control mice (Table 1A). We should acknowledge however that the urine output was calculated based on a 4 h collection period, which is a limited period to estimate the total urine output. The urinary creatinine concentration in mdx-23 mice was significantly decreased relative to the wild type (Table 1A) indicating a diluted urine output. Alternatively, the low urine creatinine concentration could be the reflection of the decreased muscle mass, which is characteristic of the mdx-23 DMD mouse model. Other established markers of glomerular and tubular injury [35], including albumin, Cystatin C, and NGAL (all expressed per ml of urine) were significantly increased in *mdx* mice relative to the age matched WT controls (2.1, 1.3, 3.4 fold respectively; $P < 0.01$) (Table 1B). In addition, the urinary levels of EGF were decreased in

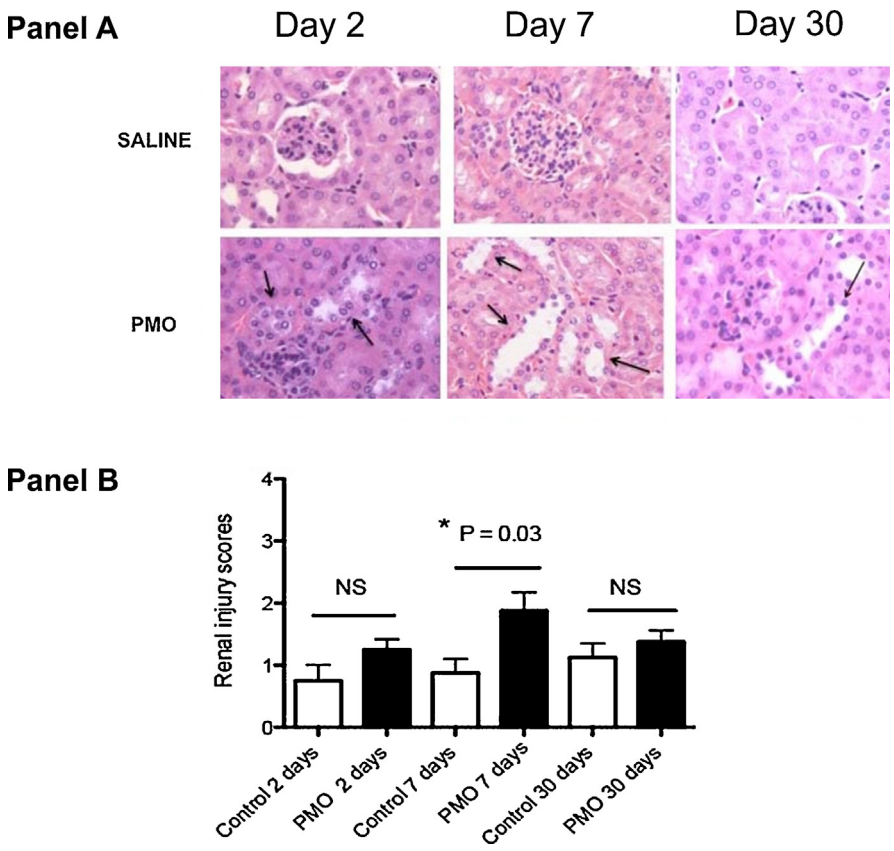

Fig. 2. (A) Histopathological changes in mdx-23 kidneys following single high dose PMO injection (800 mg/kg). Sections were prepared from mdx-23 kidneys collected at days 2, 7 and 30 following PMO or saline treatment and stained with hematoxylin and eosin stain. (Panel A) represents microscope examination (original magnification 400×) of kidney sections from representative sections. Black arrows indicate tubules that are dilated, shows signs of epithelial cell atrophy and attenuation, and/or degeneration. The more relevant renal tubular changes were observed at day 7 in PMO treated mouse but not in saline treated mouse. (Panel B) represent average quantitative data and standard deviation obtained from renal cortical tubular injury scores using a semi-quantitative scale on kidney sections from PMO treated mdx 23 ($n = 6$) and saline treated mdx-23 mice ($n = 6$) at days 2, 7 and 30 following treatment of mdx-23 mice. Significant differences were observed only at day 7 following treatment ($P = 0.03$) and less apparent at days 2 and 30 following treatment.

Table 2
Characteristics of mdx23 mice used in the study (mean ± SD).

Strain	Duration (days)	Treatment	Age (weeks)	SUn (mg/dL)	Kidney/body (g/kg)	Body weight (g)
mdx23	2	Saline ($n=6$)	8	41.43 ± 7.17	7.91 ± 0.34	28.47 ± 1.68
		PMO ($n=6$)	8	42.37 ± 5.37	7.78 ± 0.99	26.88 ± 3.09
	7	Saline ($n=6$)	7	44.89 ± 6.31	7.45 ± 0.22	25.13 ± 2.07
		PMO ($n=6$)	7	46.01 ± 2.31	7.51 ± 0.41	25.34 ± 2.29
	30	Saline ($n=6$)	11	40.00 ± 3.23	6.51 ± 0.22	33.22 ± 2.2
		PMO ($n=6$)	11	41.42 ± 3.77	6.62 ± 0.31	32 ± 1.76
P value				$P>0.05$	$P>0.05$	$P>0.05$

SUn (serum urea nitrogen), kidney to body weight, and body weight were not significantly different between PMO and saline treated mdx23 mice.

mdx-23 mice (2.0 fold decrease; $P<0.001$; Table 1B), in agreement with the results of previous AKI studies [35]. Other established urinary biomarkers of renal tubular injury, including NGAL, KIM-1, cystatin C, clusterin, GGT1, and OPN, all expressed as a ratio of the urinary creatinine values, were also significantly increased in mdx-23 mice relative to wild type mice (Table 1C). Even though KIM-1 is a well-established AKI biomarker [36–38], the KIM-1 urinary levels were only moderately increased (1.6 fold) in the 7 week old mdx-23 mice, relative to wild type mice, and when compared to the changes noted in NGAL levels (5.5 fold) under similar circumstances. We speculate that these changes are induced by the release of muscle proteins into the circulation that are filtered in the kidney. NGAL and KIM-1 may have different sensitivity to detect the chronic renal injury changes induced by proteins released by injured muscles and this is in agreement with previous report indicating that NGAL is more sensitive to AKI than KIM-1 [38]. However, further studies are needed to test this hypothesis, by assessing changes in urinary KIM-1 and NGAL at several time points throughout the progression of the muscle disease seen in mdx-23 mice. In summary, these data indicate that 7 weeks old male mdx-23 mouse develops spontaneous glomerular and tubular injury. Although the mechanism of renal injury in the mdx-23 mouse is unclear at the present time, it is tempting to speculate that these changes might be caused by the release of proteins into the circulation from injured muscles, such as myoglobin, which are filtered and accumulated in the kidney [29,39].

3.2. Renal clearance and effect of high dose PMO on the kidney histology of mdx-23 mice

Mdx-23 mice injected with a single high dose PMO (800 mg/kg) revealed a rapid urinary clearance of the drug (supplemental Fig. 2). PMO was detected in the urine as early as 30 min following the injections, and the peak urinary levels of PMO were detected 1 h following the injections. These findings are in agreement with previous PK studies [40,41], which showed that the concentration of PMO in the plasma decreases rapidly within the first 30 min after injection, and that this drop in plasma levels is correlated with rapid excretion into the urine.

In agreement with the results of previous studies [6,12], we found that mdx-23 mice injected with 800 mg/kg of PMO developed transient renal tubular injury. These lesions were characterized by the presence of single or multiple cell necrosis in renal tubular cells, and the development of mild tubular dilatation (Fig. 2), which in many cases was associated with the recruitment of inflammatory cells. A subset of PMO treated mice (<15%) showed tubular micro-cysts, and none of these mice developed proteinaceous cast. Using standard renal injury histological scores, these changes were statistically significant only in mice sacrificed 7 days after the PMO injection, compared to the control *mdx* mice ($P=0.03$), and were reversible approximately one month after the PMO injection. Interestingly, we did not find significant differences in the urinary Albumin/creatinine ratio between PMO and saline treated *mdx23* mice (supplemental Fig. S1). These findings suggest that either PMO did not induce further glomerular injury, or alternatively, that the pre-existing glomerular injury changes detected at baseline in both groups may affect the interpretation of the biomarker results (Table 2).

3.3. Pilot screening of new candidate renal injury biomarkers using SILAM proteome profiling of the kidneys of mdx-23 mice injected with high dose PMO

Molecular correlates of high dose PMO-induced acute kidney changes were identified using proteomics profiling (SILAM) in representative pair of kidney samples ($n=1$) collected at 2, 7 and 30 days after the PMO or saline injection. As shown in the supplemental Table 1, 1446 proteins were identified and quantified by at least two unique peptides per protein in mouse kidney tissues. Of the 1446 quantified proteins, 11 were found significantly altered in their levels, by two standard deviations of the average mean, in the kidneys of PMO treated-mice but not in the saline treated-mice. These 11 proteins are listed with their ratios to internal stable isotope labeled standards and fold change in PMO relative to saline treated mouse across different time points (Table 3). Most of these altered proteins were of mitochondrial origin, and involved in the oxidative reduction pathways such as cytochrome c oxidase (Cytcox), mitochondrial pyruvate carboxylase (PCB), 5-oxoprolinase (5-OPase), mitochondrial aspartate aminotransferase (mAspAT), and alpha-aminoadipic semialdehyde synthase (Aass). The expression of Annexin 2 (Anx2), a calcium-regulated membrane-binding protein, was also increased following the PMO treatment. All these proteins increased by above 2-fold at days 2 and 7 in the kidney of PMO treated mice relative to the control mice, and returned to control levels by day 30. Additional proteins showed a more delayed response, increasing 7 days after the PMO injection relative to saline; 11-fold increase in CI-B22; 3-fold increase in FABPH, Mep-1, AP-N, and AP-A. These changes returned to baseline levels by day 30.

Among the 11 proteins that were identified by the SILAM screening, eight appear to be novel candidate biomarkers of renal injury, whereas three (Mep-1, AP-N and AP-A) have been previously associated with the damage of renal proximal tubules or other renal structures [42–49]. These three proteins and other newly discovered proteins, such as FABPH and CI-B22 were further verified by western blot analysis in all PMO treated and saline treated mice ($n=6$ per group and per time point) (Fig. 3). Vincula were used as loading control, because they did not change in function of treatment and across time points. The data show that Mep-1 was slightly but significant increase at day 2 ($P<0.05$), while FABPH significantly decreased ($P<0.01$) at days 2 and 30 in kidneys of PMO treated mdx mice relative to saline treated mdx mice. CI-B22 was not significantly altered between PMO treated and untreated groups. Attempts to evaluate other discovered PMO induced proteins in the mdx mouse kidney extract (e.g. Cutco, mitochondrial PCB, 5-OPase and mitochondrial as pat) were not satisfactory due to poor quality of the commercially available antibody for these mouse proteins.

Table 3
List of proteins whose levels were significantly altered in the kidneys as a function of time following treatment of mdx23 mouse with a single high dose PMO (800 mg/kg) or saline solution alone.

Uniprot ID	Description	Day 2			Day 7			Day 30			Function
		Saline	PMO	Fold (PMO/saline)	Saline	PMO	Fold (PMO/saline)	Saline	PMO	Fold (PMO/saline)	
Q8K010	5-OPase	1.96 ± 0.09	4.96 ± 0.13	2.5	2 ± 0.12	4.98 ± 0.28	2.49	2.44 ± 0.05	2.02 ± 0.4	0.83	Catalyzes 5-oxo-L-proline to form L-glutamate, ATP to ADP
P00405	Cytcox	2.32 ± 0.6	5.56 ± 0.53	2.4	2.43 ± 0.2	7.52 ± 0.88	3.09	2.01 ± 0.17	3.6 ± 0.53	0.56	The component of the respiratory chain
Q05920	PCB	2.94 ± 0.83	6.09 ± 0.48	2.1	3.35 ± 0.05	9.65 ± 0.25	2.74	3.17 ± 0.19	2.29 ± 0.02	0.58	ATP + pyruvate + HCO_3^- = ADP + phosphate + oxaloacetate
P05202	mAspAT	1.15 ± 0.06	2.31 ± 0.09	2	1.44 ± 0.07	4.3 ± 0.69	2.99	1.94 ± 0.15	1.1 ± 0.08	0.57	Metabolite exchange between mitochondria and cytosol
Q99K67	Aass	1.54 ± 0.04	3.13 ± 0.3	2	1.63 ± 0.35	5.62 ± 0.48	3.45	2.9 ± 0.3	2.02 ± 0.09	0.70	Bifunctional enzyme
P07356	Anx2	1.37 ± 0.1	3.03 ± 0.3	2.21	1.24 ± 0	3.46 ± 0.11	2.79	3.83 ± 0.17	1.63 ± 0.12	0.44	Calcium-regulated membrane-binding protein
P16858	GAPDH	1.29 ± 0.06	2.36 ± 0.19	1.83	1.59 ± 0.13	3.73 ± 0.27	2.35	1.72 ± 0.1	1.22 ± 0.05	0.71	playing a role in glycolysis and nuclear functions
Q9CQJ8	CI-B22	2.11 ± 0.17	1.25 ± 2.9	0.78	0.89 ± 0.08	10.23 ± 0	11.49	2.92 ± 0.94	2.29 ± 0.06	0.59	Mitochondrial membrane respiratory chain NADH dehydrogenase (Complex I)
P11404	FABPH	2.22 ± 0	1.66 ± 0.02	1.08	0.44 ± 1.26	1.62 ± 0	3.68	1.93 ± 0.31	1.5 ± 0.09	0.74	A role in the intracellular transport of long-chain fatty acids and their acyl-CoA esters
P28825	MEP-1[a]	1.78 ± 0.2	2.12 ± 0.02	1.19	1.11 ± 0.98	3.55 ± 0.93	3.20	2.05 ± 0.23	1.53 ± 0.14	0.75	Kidney proximal tubules intestinal brush borders and salivary ducts
P97449	AP-N[a]	2.09 ± 0.07	3.47 ± 0.08	1.66	2.03 ± 0.36	6.61 ± 0.85	3.26	2.41 ± 0.22	1.66 ± 0.01	0.68	proximal convoluted tubules
P16406	AP-A[a]	1.64 ± 0	3.07 ± 2.82	0.70	1.87 ± 0.22	6.51 ± 0.03	3.48	2.04 ± 0.03	1.43 ± 0.04	1.87	A role in the catabolic pathway of the renin-angiotensin system

Top row indicates the days after single injection of high dose PMO or saline solutions. *Abbreviations*: 5-OPase for 5-oxoprolinase; Cytcox for Cytochrome c oxidase subunit 2; PCB for mitochondrial pyruvate carboxylase; mAspAT for mitochondrial aspartate aminotransferase; GAPDH for glyceraldehyde-3-phosphate dehydrogenase; Aass for alpha-aminoadipic semialdehyde synthase; Anx2 for annexin 2; CI-B22 for NADH dehydrogenase [ubiquinone] 1 beta subcomplex subunit 9; FABPH for fatty acid binding protein heart type; AP-N for aminopeptidase N; AP-A for glutamyl aminopeptidase; Mep-1 for Meprin A subunit alpha; PMO: phosphorodiamidate morpholino oligomer. Data are presented as mean ± standard deviation of $n = 1$ per group and per time point. The means ± SD represent the average of light to heavy isotope ratio values obtained for all peptides detected for each protein in each sample.

[a] Known biomarkers associated with kidney injury.

Table 4A
List of urinary proteins significantly altered by LC–MS/MS with SILAM in their levels as a function of time following single high dose PMO (800 mg/kg) or saline injection of mdx-23 mouse.

Uniprot ID	Description	Day 1			Day 6			Day 29		
		Saline	PMO	PMO/saline	Saline	PMO	PMO/saline	Saline	PMO	PMO/saline
P01132	EGF	2.65 ± 0.46	3.13 ± 0.21	1.18	0.93 ± 0.02	2.47 ± 0.15	#2.66	1.58 ± 0.07	1.68 ± 0.86	1.06
Q06890	Clusterin	2.15 ± 0.6	4.16 ± 0.16	#1.93	1.39 ± 0.13	1.72 ± 0.01	1.23	1.03 ± 0.21	1.15 ± 0.29	1.12
P00688	AMY2	2.19 ± 0	10.07 ± 1.3	#4.60	2.76 ± 0.01	2.83 ± 0.32	1.02	3.21 ± 0	3.37 ± 0.08	1.04
Q60928	GGT 1	x	3.82	Unique	0.88 ± 0.08	0.84 ± 0.01	0.95	0.98 ± 0.55	4.15 ± 0	#4.23
P97449	AP-N	x	2.93	Unique	1.49 ± 0.02	1.6 ± 0.1	1.07	1.45 ± 0.04	3.16 ± 2.98	#2.17

Abbreviations: EGF, epidermal growth factor; AMY2, pancreatic alpha-amylase; GGT1, gamma-glutamyltranspeptidase; AP-N, aminopeptidase N, X, not determined; PMO, phosphorodiamidate morpholino oligomer. The means ± SD represent the average of light to heavy isotope ratio values obtained for all peptides detected for each protein in each sample; sample used $n = 1$.

# indicates detected urinary proteins increased fold ≥ .5 in PMO vs saline.

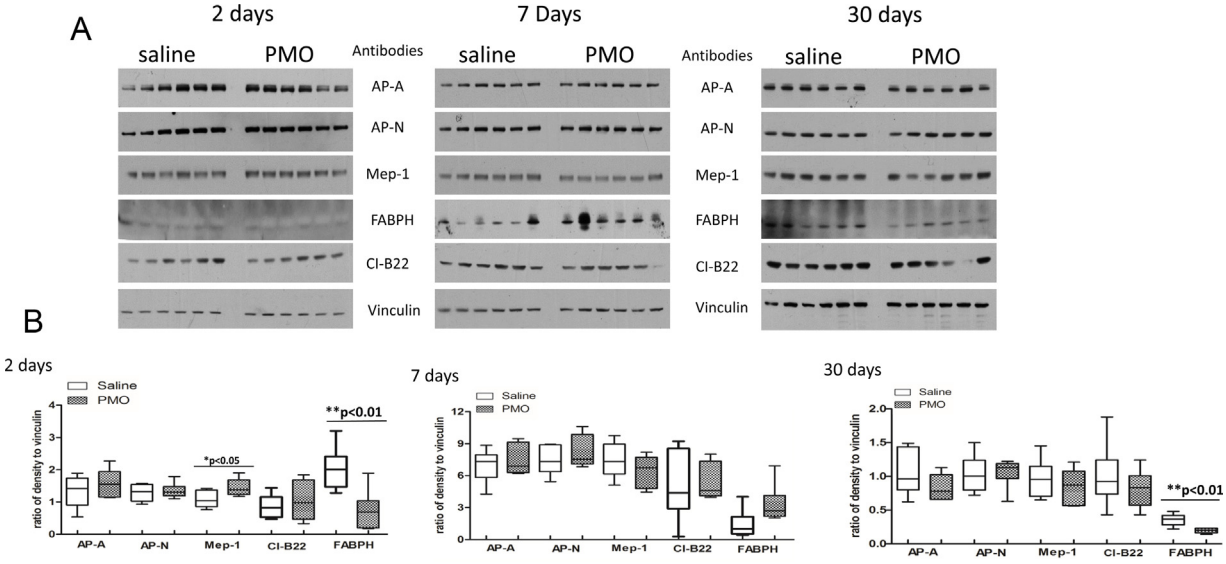

Fig. 3. Western blot verification of candidate proteins that were found altered in their levels in kidney proteome screening of PMO treated mdx-23 mice relative to saline treated mice. Five protein candidates: Aminopeptidase N(AP-N), Meprin A subunit alpha (Mep-1), glutamyl aminopeptidase (AP-A), Fatty acid binding protein heart type (FABPH), NADH dehydrogenase [ubiquinone] 1 beta subcomplex subunit 9 [CI-B22] that were found altered in their levels in the kidneys of PMO treated mdx-23 mouse kidney relative to saline treated mdx-23 mouse ($n = 6$ per group and per time point) were targeted for western-blot analysis. (Panel 3A) shows immunochemical blot of all proteins (AP-A, AP-N, Mep-1, FABPH, CI-B22, and vinculin were used as loading controls) in each group and each time point. Panel 3B shows statistical box plots analysis for each protein in each group and each time point, empty box represents saline treated group, and pattern box represents PMO treated group. Each box indicates mean and standard error obtained from 6 samples. *P* values are indicated on the top of each graph. Mep-1 significantly increased at day 2, FABPH significantly decreased at days 2 and 30.

3.4. Pilot screening of new candidate renal injury biomarkers using SILAM proteome of urine samples collected from mdx-23 mice injected with high dose PMO

For a more in depth pilot screening of new potential candidate urinary biomarkers associated with the renal PMO load and clearance, we performed SILAM proteome profiling on longitudinal urine samples collected from *mdx-23* mice at 1, 6 and 29 days after a single dose of PMO (800 mg/kg). Matched time series samples from saline injected mdx-23 mice were used as controls. A single representative pair of treated and untreated mouse was randomly chosen for each time point using the proteome profiling SILAM approach. In this discovery phase, 147 proteins were identified and quantified across all mice and time points analyzed (supplemental Table 2). The majority of proteins detected in urine were either secreted proteins (38% of total) or membrane-associated proteins (20%) (Fig. 4). Only 5 proteins among the 147 quantified urinary proteins showed significant alterations in their levels over time in PMO-injected mouse relative to saline injected mouse (Table 4A). Among these, clusterin and AMY2 increased by 1.9 and 4.6 fold respectively at day 1 in urine of PMO treated mouse relative to saline treated mouse, and then returned to normal levels at days 6 and 29 following treatment. EGF increased at day 6 by 2.6 fold in PMO treated mouse relative to saline treated mouse. At day 29 post treatment, AP-N and GGT1 increased by 2.2- and 4.2-fold respectively in PMO treated mouse relative to saline treated mouse. Normalization to creatinine levels did not change the interpretation of the data expressed as a ratio of the urinary creatinine concentration in fold changes (Table 4B).

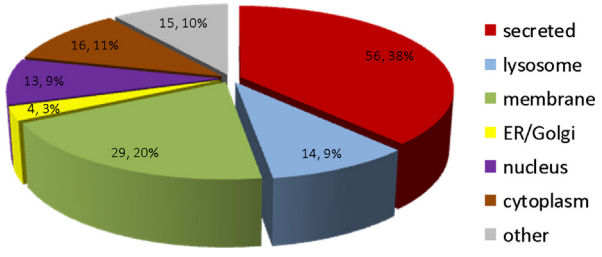

Fig. 4. Subcellular localization of proteins identified in urine samples of mdx-23 mouse. An average of 147 proteins were identified and quantified in urine samples from mdx-23 mice. Among these, 38% (56 proteins) were secreted proteins; 20% (29 proteins) membrane origin; 9% (14 proteins) lysosomal origin, 3% (4 proteins) ER/Golgi origin; 9% (13 proteins) nucleus origin, 11% (16 proteins) cytosolic, and 10% (15 proteins) of unspecified origin. Subcelular localization was retrieved from Uniprot knowledge database.

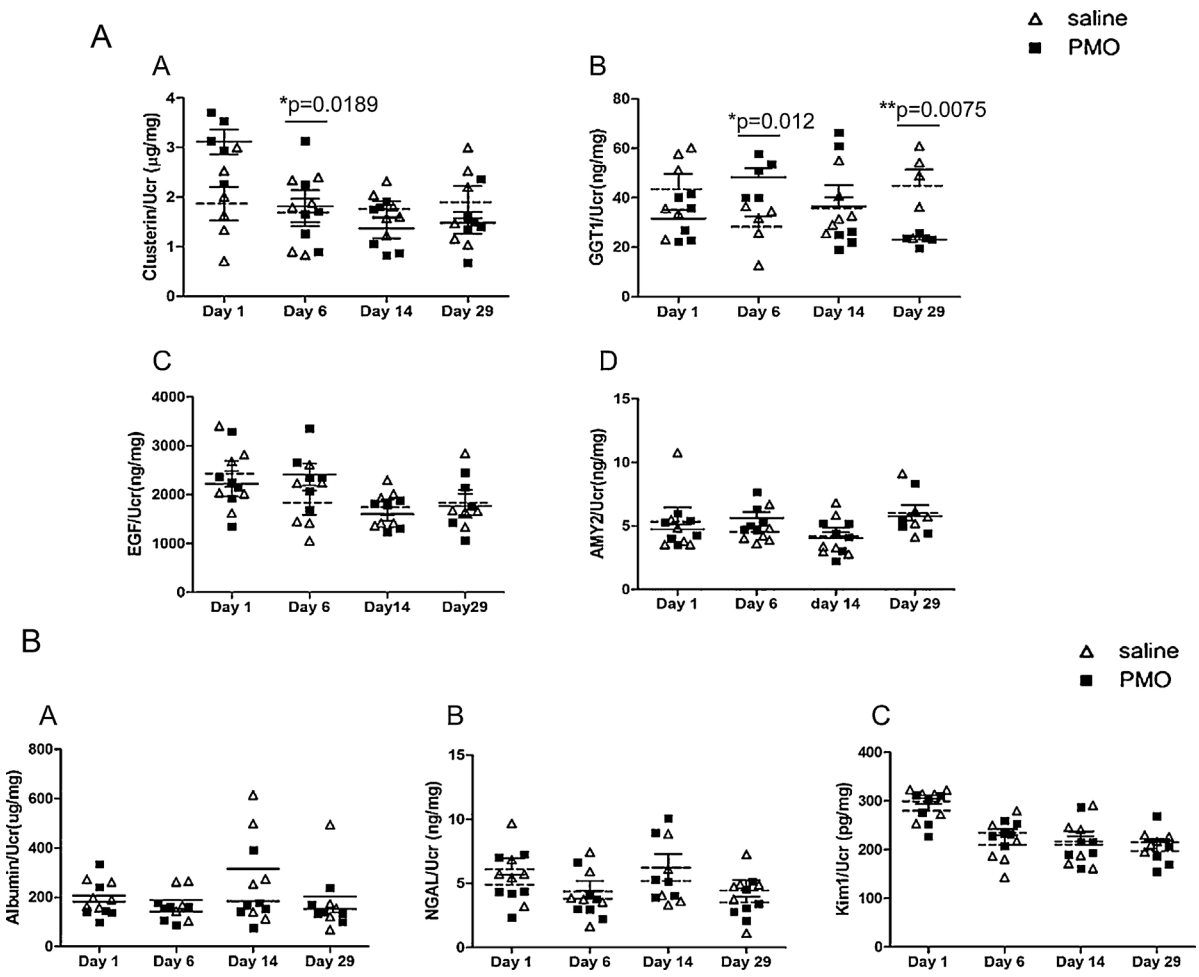

Fig. 5. Evaluation of biomarkers associated with PMO renal load and clearance in urine samples of single high dose PMO injected mdx-23 mice. Potential urinary biomarkers associated with PMO renal load and clearance that were identified by differential proteome profiling of urine samples collected at days 1, 6, 14 and 29 following treatment of mdx-23 with single high dose PMO (800 mg/kg) or saline solution alone were targeted for an evaluation, using ELISA assays, in all PMO and saline treated mdx-23 ($n = 6$ per group and per time point). (A) Plots are shown from top row to bottom left to right for clusterin, GGT1 (gamma glutamyltranspeptidase 1), EGF (pro-epidermal growth factor), and AMY2 (pancreatic alpha-amylase) discovered in this study. (B) Shows plots for three known AKI biomarkers including Albumin, NGAL (Neutrophil gelatinase-associated lipocalin) and KIM-1 (Kidney Injury Molecule-1). All data were normalized by urine creatinine levels. Significant differences between PMO treated group (solid squares) and saline treated group (empty triangles) are indicated by * or ** on the top of each plot and respective Ps.

These results were further verified in urine samples collected from all mdx-23 mice injected with either with PMO or saline ($n = 6$ per group and per time point) using well established ELISA assays. Only clusterin and GGT1 were found significantly increased at days 1 and 6 respectively in the PMO treated group relative to the control group (Fig. 5A). Interestingly, targeted analysis by ELISA assay of some known AKI biomarkers that we found already elevated in urine of mdx-23 mice relative to wild type mice at baseline (see data above Tables 1B and 1C) did not show any further increase in PMO injected mdx-23 mice relative to saline injected mdx controls (Fig. 5B). Given the pre-exiting renal injury detected at baseline in all mdx-23 mice, our findings suggest that clusterin and GGT1 might be specific candidate biomarkers to detect the PMO-induced renal tubular injury, even in the context of underlying renal damage.

Table 4B
Fold change of selected urinary biomarkers in PMO treated relative to saline treated mdx-23 mice in Table 4A after normalization to creatinine levels.

UniProt ID	Description	Day 1 PMO/Saline	Day 6 PMO/saline	Day 30 PMO/saline
P01132	EGF	1.29	[a]3.82	0.69
Q06890	Clusterin	[a]2.11	[a]1.71	0.72
P00688	AMY2	[a]5.00	1.38	0.68
Q60928	GGT1	Unique	1.17	[a]2.74
P97449	AP-N	Unique	[a]1.5	1.41

[a] Biomarkers increased in PMO treatment, folds > 1.5. Unique: only determined in PMO.

4. Discussion

The mdx-23 mouse model has been utilized extensively to study the pathogenesis and treatment of DMD, including pre-clinical studies of therapeutic oligonucleotide-induced exon skipping of the *DMD* gene to restore dystrophin protein expression in muscle [50,51]. Because previous pre-clinical studies showed that this gene therapy approach can cause renal tubular injury [6,12], we carried out this pilot study to identify new candidate urinary biomarkers of AKI in the mdx-23 mouse injected with high dose PMO, using a proteomic profiling SILAM-approach. Surprisingly, we found that adult mdx-23 mice developed spontaneous renal injury independently of the PMO injection. These changes were manifested by albuminuria, increased urine output, and changes in several established urinary biomarkers of acute kidney injury (AKI). Nonetheless, a single high dose PMO injection induced further renal tubular injury in 7 week old mdx-23 mice, which peaked at 7 days, and

returned to the baseline levels at 30 days. The SILAM approach identified specific changes in the expression of several proteins, including Mep-1 in kidneys, clusterin and GGT1 in urine, which were validated by Western blots or ELISA and may become promising candidate biomarkers to monitor the renal outcome of patients with DMD in future human clinical trials.

As discussed above, we sought to identify potential urinary biomarkers to monitor the accumulation of oligonucleotides in proximal tubules of mice that could be transitioned to clinically useful biomarkers in human clinical trials of therapeutic oligonucleotides drug treatments. Unfortunately we were unable to compare other oligonucleotides containing the phosphorothioate backbone chemistry because of the toxicity of these molecules when given at high doses. One remarkable finding of our study was the discovery of pre-existing renal injury in the mdx-23 mouse, relative to the wild type control mouse. These findings should be taken into consideration to interpret the results and to determine their clinical translational value of our findings for patients with DMD. More specifically, in the urinary proteome of the mdx-23 mouse at baseline, we found elevated levels of albumin, cystatin C, NGAL, and increased urine output. Although the mechanisms responsible for the renal injury are not understood at the present time, there are two possible interpretations of these data. First, it is possible that dystrophin-deficiency in kidney cells directly induces kidney dysfunction, leading to proteinuria in the *mdx-23* mice [52,53]. Indeed, dystrophin is expressed in smooth muscle, including vascular smooth muscle [52,53], and the dystrophin-dystroglycan complex may play a role in maintaining vasculature and kidney function [54]. Second, dystrophin is best characterized as an important component of the myofiber membrane cytoskeleton in skeletal muscle. Its lack of expression in Duchenne leads to muscle tissue damage and high protein loads of muscle-derived components, such as creatine kinase and myoglobin into blood circulation. Furthermore, extensive muscle damage (rhabdomyolysis) leads to myoglobinurea and can cause severe acute kidney damage with subsequent kidney failure. It is plausible that the chronic leakage of myofiber components from muscle tissue into blood in the mdx-23 mouse model leads to a chronic mild kidney damage and the proteinuria we describe. The reported susceptibility of both DMD patients and the mdx-23 mouse to bouts of myoglobinuria may be consistent with this model [55]. These two models are not mutually exclusive. We note that kidney failure is not a typical feature of Duchenne muscular dystrophy or the mdx mouse model. Thus, it appears that the changes detected are not progressive. Further studies are needed to explore the pathogenesis of these lesions.

It is worth mentioning that the dose of PMO utilized in our study was 16–25 times higher than the doses used in clinical trials [13,14]. This PMO dose induced transient renal tubular histological changes, which peaked 7 days after injection, without causing acute renal failure, and returned to baseline levels 30 days after the injection. These data are in agreement with the results of previous studies done in mdx mice injected weekly with high dose PMO (960 mg/kg) for up to 12 weeks [6]. Interestingly, several biomarkers of AKI that were increased at baseline in the urine of mdx mice relative to wild type mice, remained unchanged in PMO-treated mice throughout the study time points (e.g. 1, 6, 14 and 29 days). It is possible that the renal injury changes detected at baseline, which were not homogenous in all mice, could affect our ability to interpret the biomarker results. Nonetheless, the SILAM data together with the renal histological findings indicate that PMO induced further renal tubular injury, which is transient and appears to be reversible.

Query of the molecular profiles of both the kidney and urinary proteome found a limited number of PMO-induced changes that could be associated with the transient oligonucleotide accumulation in renal tubular cells. The clinical relevance of these findings for patients receiving PMO therapy is unclear, since the murine dose administered was over 25 fold higher than the expected human dose given in the clinic. In the kidney, we observed changes in known AKI associated proteins such as Mep-1 [42–44] at day 2 ($P < 0.05$), and FABPH [56–59] at day 7 even though not significant (Fig. 3B, $P = 0.06$). These changes occurred as early as day 2 following PMO injection, and before the most severe renal histological changes were detected in mice treated with PMO. Finally, the proteomic profiling SILAM approaches in kidney samples shows that all these changes returned to baseline levels 30 days after the PMO injection.

In the urinary proteome, of the 147 quantified proteins only clusterin and GGT1 showed significant alterations both via proteomics and ELISA evaluation. Other known AKI biomarkers did not show a PMO-induced increase in urine. While clusterin was increased in urine of PMO treated mdx mice as early as 24 h post treatment, GGT1 was increased at day 6 post treatment. Both proteins returned to normal levels at day 14 following treatment. Clusterin is a secreted chaperone protein that is involved in the regeneration and proliferation of tubular epithelial cells, progression of the cell cycle, and reparation of DNA damage [60–62]. Increased levels of urinary clusterin have been reported to be a sensitive and specific marker to monitor drug-induced insults on renal tubules [63]. This early increase in clusterin expression was associated with later tubular recovery, as evidenced by experiments performed on clusterin KO mice vs. wild type mice. Taken together, these findings suggest that urinary clusterin could be used as readout to monitor both kidney insult and recovery.

GGT1, a tubular brush border enzyme, was shown in this study to be elevated in the urine of PMO treated mice, relative to saline treated mice at day 6 by ELISA assays. This data is in agreement with previous studies where it has been shown that the urinary levels of GGT1 increased immediately after kidney ischemia-reperfusion insult, and then declined with time with other AKI biomarkers [64–66]. Other studies have used urinary levels of GGT1 as an indicator of proximal tubular injury in rats injected with high doses of colistin [67] or cisplatin [68]. Our finding that GGT1 increased in urine at day 6 post injection in PMO treated mice relative to saline treated mice correlated with the changes seen in the morphology of proximal tubules that occurred at day 7 in PMO treated mice and is in agreement with previous studies above. Interestingly, urinary GGT1 returned to normal levels at 14 days following PMO injection and even decreased by almost 2 fold at day 29 when compared to the urinary levels detected in saline treated mdx mice. According to efficiency study of morpholino-induced exon skipping [50] in mdx mice, it showed dystrophin restoration and muscle improvement at about day 14 following PMO treatment. It is plausible that recovery of PMO treated mdx mice from muscular dystrophin imply less muscle necrosis and thus less stress on kidneys and thus GGT1 was further decreased in PMO rescued mdx-23 relative to saline treated mdx-23. However this hypothesis remains to be verified using different PMO regimens and efficacy studies.

Even though the increase in the urine levels of clusterin and GGT1 was moderate at days 1 and 6 respectively in PMO relative to saline treated group these alterations could still serve as marker to monitor PMO kidney load. However, these preliminary data need to be validated in future studies using chronic treatment of PMO for longer period and in larger sample size.

5. Conclusions

In summary, we found that mdx-23 mice can develop spontaneous renal injury, and that these changes may affect the identification of new biomarkers, as well as the outcome of mice treated with PMO. Nonetheless, using a combination of the SILAM

approach and ELISA, we have identified at least two new potential candidate urinary biomarkers that appear to be associated with the renal PMO load, clearance, and the development of transient renal tubular injury. Previous studies [41], including our current data, show that urinary PMO clearance occurs immediately after injection and peaks at about 1 h post injection. Urinary levels of clusterin followed the PMO clearance trend. It increased in urine during the first 24 h then returned to normal levels at days 6 and 29 post injection suggesting rapid kidney recovery from high dose PMO. GGT1 on the other hand, increased at day 6 in urine following the PMO injection, and then returned to normal levels at day 14 post treatment. Increase in clusterin levels seem to be beneficial to kidneys (e.g. renal proximal tubule protection and repair) as demonstrated in previous studies [61] while increased levels of GGT1 seems to indicate the presence of proximal tubular injury, as demonstrated in cisplatin treated rats [69]. Thus clusterin and GGT1 appear to be promising urinary candidate biomarkers to monitor the early stages of renal proximal tubular injury induced by PMO and other oligonucleotides. Further studies are warranted to validate these findings in patients treated with PMO.

Acknowledgements

This work was supported by the National Institutes of Health grant U54HD07160, and partially supported by NIH core grants 2R24HD050846-06 (National Center for Medical Rehabilitation Research), R01 DK-049419 and UL1RR031988 (CTSI-CN). The authors would like to thank Dr. Peter Sazani and Dr. Edward M Kaye for revising the manuscript and for their valuable inputs and suggestions.

Appendix A. Supplementary data

Supplementary data associated with this article can be found, in the online version, at doi:10.1016/j.toxrep.2015.05.008

References

[1] R.Z. Yu, J.S. Grundy, R.S. Geary, Clinical pharmacokinetics of second generation antisense oligonucleotides, Expert Opin. Drug Metab. Toxicol. 9 (2013) 169–182.
[2] A.L. Southwell, N.H. Skotte, C.F. Bennett, M.R. Hayden, Antisense oligonucleotide therapeutics for inherited neurodegenerative diseases, Trends Mol. Med. 18 (2012) 634–643.
[3] T.A. Zanardi, S.C. Han, E.J. Jeong, S. Rime, R.Z. Yu, K. Chakravarty, S.P. Henry, Pharmacodynamics and subchronic toxicity in mice and monkeys of ISIS 388626, a second-generation antisense oligonucleotide that targets human sodium glucose cotransporter 2, J. Pharmacol. Exp. Ther. 343 (2012) 489–496.
[4] S.P. Henry, M. Johnson, T.A. Zanardi, R. Fey, D. Auyeung, P.B. Lappin, A.A. Levin, Renal uptake and tolerability of a 2′-O-methoxyethyl modified antisense oligonucleotide (ISIS 113715) in monkey, Toxicology 301 (2012) 13–20.
[5] E.W. Alton, H.A. Boushey, H. Garn, F.H. Green, M. Hodges, R.J. Martin, R.D. Murdoch, H. Renz, S.B. Shrewsbury, R. Seguin, G. Johnson, J.D. Parry, J. Tepper, P. Renzi, J. Cavagnaro, N. Ferrari, Clinical expert panel on monitoring potential lung toxicity of inhaled oligonucleotides: consensus points and recommendations, Nucleic Acid Ther. 22 (2012) 246–254.
[6] P. Sazani, K.P. Ness, D.L. Weller, D. Poage, K. Nelson, A.S. Shrewsbury, Chemical and mechanistic toxicology evaluation of exon skipping phosphorodiamidate morpholino oligomers in mdx mice, Int. J. Toxicol. 30 (2011) 322–333.
[7] C.L. Berman, K. Cannon, Y. Cui, D.J. Kornbrust, A. Lagrutta, S.Z. Sun, J. Tepper, G. Waldron, H.S. Younis, Recommendations for safety pharmacology evaluations of oligonucleotide-based therapeutics, Nucleic Acid Ther. 24 (2014) 291–301.
[8] M.A. Hallett, P. Dalal, T.W. Sweatman, T. Pourmotabbed, The distribution, clearance, and safety of an anti-MMP-9 DNAzyme in normal and MMTV-PyMT transgenic mice, Nucleic Acid Ther. 23 (2013) 379–388.
[9] S.A. Burel, S.R. Han, H.S. Lee, D.A. Norris, B.S. Lee, T. Machemer, S.Y. Park, T. Zhou, G. He, Y. Kim, A.R. MacLeod, B.P. Monia, S. Lio, T.W. Kim, S.P. Henry, Preclinical evaluation of the toxicological effects of a novel constrained ethyl modified antisense compound targeting signal transducer and activator of transcription 3 in mice and cynomolgus monkeys, Nucleic Acid Ther. 23 (2013) 213–227.
[10] M. Dirin, J. Winkler, Influence of diverse chemical modifications on the ADME characteristics and toxicology of antisense oligonucleotides, Expert Opin. Biol. Ther. 13 (2013) 875–888.
[11] P. Sazani, D.L. Weller, S.B. Shrewsbury, Safety pharmacology and genotoxicity evaluation of AVI-4658, Int. J. Toxicol. 29 (2010) 143–156.
[12] P. Sazani, K.P. Ness, D.L. Weller, D.W. Poage, K. Palyada, S.B. Shrewsbury, Repeat-dose toxicology evaluation in cynomolgus monkeys of AVI-4658, a phosphorodiamidate morpholino oligomer (PMO) drug for the treatment of duchenne muscular dystrophy, Int. J. Toxicol. 30 (2011) 313–321.
[13] J.R. Mendell, L.R. Rodino-Klapac, Z. Sahenk, K. Roush, L. Bird, L.P. Lowes, L. Alfano, A.M. Gomez, S. Lewis, J. Kota, V. Malik, K. Shontz, C.M. Walker, K.M. Flanigan, M. Corridore, J.R. Kean, H.D. Allen, C. Shilling, K.R. Melia, P. Sazani, J.B. Saoud, E.M. Kaye, Eteplirsen for the treatment of Duchenne muscular dystrophy, Ann. Neurol. 74 (2013) 637–647.
[14] S. Cirak, V. Arechavala-Gomeza, M. Guglieri, L. Feng, S. Torelli, K. Anthony, S. Abbs, M.E. Garralda, J. Bourke, D.J. Wells, G. Dickson, M.J. Wood, S.D. Wilton, V. Straub, R. Kole, S.B. Shrewsbury, C. Sewry, J.E. Morgan, K. Bushby, F. Muntoni, Exon skipping and dystrophin restoration in patients with Duchenne muscular dystrophy after systemic phosphorodiamidate morpholino oligomer treatment: an open-label, phase 2, dose-escalation study, Lancet 378 (2011) 595–605.
[15] M. Kinali, V. Arechavala-Gomeza, L. Feng, S. Cirak, D. Hunt, C. Adkin, M. Guglieri, E. Ashton, S. Abbs, P. Nihoyannopoulos, M.E. Garralda, M. Rutherford, C. McCulley, L. Popplewell, I.R. Graham, G. Dickson, M.J. Wood, D.J. Wells, S.D. Wilton, R. Kole, V. Straub, K. Bushby, C. Sewry, J.E. Morgan, F. Muntoni, Local restoration of dystrophin expression with the morpholino oligomer AVI-4658 in Duchenne muscular dystrophy: a single-blind, placebo-controlled, dose-escalation, proof-of-concept study, Lancet Neurol. 8 (2009) 918–928.
[16] E.P. Hoffman, E.M. McNally, Exon-skipping therapy: a roadblock, detour, or bump in the road? Sci. Transl. Med. 6 (2014) 230fs214.
[17] E.P. Hoffman, A. Bronson, A.A. Levin, S. Takeda, T. Yokota, A.R. Baudy, E.M. Connor, Restoring dystrophin expression in duchenne muscular dystrophy muscle progress in exon skipping and stop codon read through, Am. J. Pathol. 179 (2011) 12–22.
[18] J. Alter, F. Lou, A. Rabinowitz, H. Yin, J. Rosenfeld, S.D. Wilton, T.A. Partridge, Q.L. Lu, Systemic delivery of morpholino oligonucleotide restores dystrophin expression bodywide and improves dystrophic pathology, Nat. Med. 12 (2006) 175–177.
[19] B. Wu, H.M. Moulton, P.L. Iversen, J. Jiang, J. Li, J. Li, C.F. Spurney, A. Sali, A.D. Guerron, K. Nagaraju, T. Doran, P. Lu, X. Xiao, Q.L. Lu, Effective rescue of dystrophin improves cardiac function in dystrophin-deficient mice by a modified morpholino oligomer, Proc. Natl. Acad. Sci. U. S. A. 105 (2008) 14814–14819.
[20] S. Fletcher, K. Honeyman, A.M. Fall, P.L. Harding, R.D. Johnsen, S.D. Wilton, Dystrophin expression in the mdx mouse after localised and systemic administration of a morpholino antisense oligonucleotide, J. Gene Med. 8 (2006) 207–216.
[21] T. Yokota, Q.L. Lu, T. Partridge, M. Kobayashi, A. Nakamura, S. Takeda, E. Hoffman, Efficacy of systemic morpholino exon-skipping in Duchenne dystrophy dogs, Ann. Neurol. 65 (2009) 667–676.
[22] S. Campion, J. Aubrecht, K. Boekelheide, D.W. Brewster, V.S. Vaidya, L. Anderson, D. Burt, E. Dere, K. Hwang, S. Pacheco, J. Saikumar, S. Schomaker, M. Sigman, F. Goodsaid, The current status of biomarkers for predicting toxicity, Expert Opin. Drug Metab. Toxicol. 9 (2013) 1391–1408.
[23] S. Alvarez, C. Suazo, A. Boltansky, M. Ursu, D. Carvajal, G. Innocenti, A. Vukusich, M. Hurtado, S. Villanueva, J.E. Carreno, A. Rogelio, C.E. Irarrazabal, Urinary exosomes as a source of kidney dysfunction biomarker in renal transplantation, Transplant. Proc. 45 (2013) 3719–3723.
[24] C. Fagundes, M.N. Pepin, M. Guevara, R. Barreto, G. Casals, E. Sola, G. Pereira, E. Rodriguez, E. Garcia, V. Prado, E. Poch, W. Jimenez, J. Fernandez, V. Arroyo, P. Gines, Urinary neutrophil gelatinase-associated lipocalin as biomarker in the differential diagnosis of impairment of kidney function in cirrhosis, J. Hepatol. 57 (2012) 267–273.
[25] M.Y. Hong, C.C. Tseng, C.C. Chuang, C.L. Chen, S.H. Lin, C.F. Lin, Urinary macrophage migration inhibitory factor serves as a potential biomarker for acute kidney injury in patients with acute pyelonephritis, Mediat. Inflamm. 2012 (2012) 381358.
[26] A. Kamijo, T. Sugaya, A. Hikawa, M. Yamanouchi, Y. Hirata, T. Ishimitsu, A. Numabe, M. Takagi, H. Hayakawa, F. Tabei, T. Sugimoto, N. Mise, M. Omata, K. Kimura, Urinary liver-type fatty acid binding protein as a useful biomarker in chronic kidney disease, Mol. Cell. Biochem. 284 (2006) 175–182.
[27] Y. Togashi, Y. Miyamoto, Urinary cystatin C as a biomarker for diabetic nephropathy and its immunohistochemical localization in kidney in Zucker diabetic fatty (ZDF) rats, Exp. Toxicol. Pathol. 65 (2013) 615–622.
[28] D.B. McClatchy, L. Liao, S.K. Park, T. Xu, B. Lu, J.R. Yates Iii, Differential proteomic analysis of mammalian tissues using SILAM, PLoS ONE 6 (2011) e16039.
[29] Y. Hathout, R.L. Marathi, S. Rayavarapu, A. Zhang, K.J. Brown, H. Seol, H. Gordish-Dressman, S. Cirak, L. Bello, K. Nagaraju, T. Partridge, E.P. Hoffman, S. Takeda, J.K. Mah, E. Henricson, C. McDonald, Discovery of serum protein biomarkers in the mdx mouse model and cross-species comparison to Duchenne muscular dystrophy patients, Hum. Mol. Genet. 23 (2014) 6458–6469.
[30] B.T. Kurien, N.E. Everds, R.H. Scofield, Experimental animal urine collection: a review, Lab. Anim. 38 (2004) 333–361.
[31] P.C. Mattison, A.A. Soler-García, J.R. Das, M. Jerebtsova, S. Perazzo, P. Tang, P.E. Ray, Role of circulating fibroblast growth factor-2 in lipopolysaccharide-induced acute kidney injury in mice, Pediatr. Nephrol. 27 (2012).
[32] D. Schnell, M. Reynaud, M. Venot, A.L. Le Maho, M. Dinic, M. Baulieu, G. Ducos, J. Terreau, F. Zeni, E. Azoulay, F. Meziani, J. Duranteau, M. Darmon, Resistive

index or color-doppler semi-quantitative evaluation of renal perfusion by inexperienced physicians: results of a pilot study, Minerva Anestesiol. 80 (2014) 1273–1281.
[33] A. Oda, K. Morozumi, K. Uchida, Histological factors of 1-h biopsy influencing the delayed renal function and outcome in cadaveric renal allografts, Clin. Transplant. 13 (Suppl. 1) (1999) 6–12.
[34] D.N. Gilbert, C. Plamp, P. Starr, W.M. Bennet, D.C. Houghton, G. Porter, Comparative nephrotoxicity of gentamicin and tobramycin in rats, Antimicrob. Agents Chemother. 13 (1978) 34–40.
[35] S.B. Hoffman, A.N. Massaro, A.A. Soler-Garcia, S. Perazzo, P.E. Ray, A novel urinary biomarker profile to identify acute kidney injury (AKI) in critically ill neonates: a pilot study, Pediatr. Nephrol. 28 (2013) 2179–2188.
[36] Q.H. Luo, M.L. Chen, F.J. Sun, Z.L. Chen, M.Y. Li, W. Zeng, L. Gong, A.C. Cheng, X. Peng, J. Fang, L. Tang, Y. Geng, KIM-1 and NGAL as biomarkers of nephrotoxicity induced by gentamicin in rats, Mol. Cell. Biochem. 397 (2014) 53–60.
[37] V. Sinha, L.M. Vence, A.K. Salahudeen, Urinary tubular protein-based biomarkers in the rodent model of cisplatin nephrotoxicity: a comparative analysis of serum creatinine, renal histology, and urinary KIM-1, NGAL, and NAG in the initiation, maintenance, and recovery phases of acute kidney injury, J. Investig. Med. 61 (2013) 564–568.
[38] M. Mussap, A. Noto, V. Fanos, J.N. Van Den Anker, Emerging biomarkers and metabolomics for assessing toxic nephropathy and acute kidney injury (AKI) in neonatology, BioMed Res. Int. (2014) 602526.
[39] T. Matsumura, T. Saito, H. Fujimura, S. Sakoda, [Renal dysfunction is a frequent complication in patients with advanced stage of Duchenne muscular dystrophy], Rinsho shinkeigaku 52 (2012) 211–217.
[40] A. Amantana, H.M. Moulton, M.L. Cate, M.T. Reddy, T. Whitehead, J.N. Hassinger, D.S. Youngblood, P.L. Iversen, Pharmacokinetics, biodistribution, stability and toxicity of a cell-penetrating peptide-morpholino oligomer conjugate, Bioconjug. Chem. 18 (2007) 1325–1331.
[41] V. Arora, G.R. Devi, P.L. Iversen, Neutrally charged phosphorodiamidate morpholino antisense oligomers: uptake, efficacy and pharmacokinetics, Curr. Pharm. Biotechnol. 5 (2004) 431–439.
[42] G.P. Kaushal, R.S. Haun, C. Herzog, S.V. Shah, Meprin A metalloproteinase and its role in acute kidney injury, Am. J. Physiol. Ren. Physiol. 304 (2013) F1150–F1158.
[43] R.E. Yura, S.G. Bradley, G. Ramesh, W.B. Reeves, J.S. Bond, Meprin A metalloproteases enhance renal damage and bladder inflammation after LPS challenge, Am. J. Physiol. Ren. Physiol. 296 (2009) F135–F144.
[44] C. Herzog, R. Seth, S.V. Shah, G.P. Kaushal, Role of meprin A in renal tubular epithelial cell injury, Kidney Int. 71 (2007) 1009–1018.
[45] R. Mathew, S. Futterweit, E. Valderrama, A.A. Tarectecan, J.E. Bylander, J.S. Bond, H. Trachtman, Meprin-alpha in chronic diabetic nephropathy: interaction with the renin-angiotensin axis, Am. J. Physiol. Ren. Physiol. 289 (2005) F911–F921.
[46] S. Carmago, S.V. Shah, P.D. Walker, Meprin, a brush-border enzyme, plays an important role in hypoxic/ischemic acute renal tubular injury in rats, Kidney Int. 61 (2002) 959–966.
[47] P.D. Walker, G.P. Kaushal, S.V. Shah, Meprin A, the major matrix degrading enzyme in renal tubules, produces a novel nidogen fragment in vitro and in vivo, Kidney Int. 53 (1998) 1673–1680.
[48] A. Quesada, F. Vargas, S. Montoro-Molina, F. O'Valle, M.D. Rodriguez-Martinez, A. Osuna, I. Prieto, M. Ramirez, R. Wangensteen, Urinary aminopeptidase activities as early and predictive biomarkers of renal dysfunction in cisplatin-treated rats, PLoS ONE 7 (2012) e40402.
[49] M. Nomura, S. Nomura, T. Mitsui, M. Suzuki, H. Kobayashi, T. Ito, A. Itakura, F. Kikkawa, S. Mizutani, Possible involvement of aminopeptidase A in hypertension and renal damage in Dahl salt-sensitive rats, Am. J. Hypertens. 18 (2005) 538–543.
[50] B. Wu, P. Lu, E. Benrashid, S. Malik, J. Ashar, T.J. Doran, Q.L. Lu, Dose-dependent restoration of dystrophin expression in cardiac muscle of dystrophic mice by systemically delivered morpholino, Gene Ther. 17 (2010) 132–140.
[51] B. Wu, H.M. Moulton, P.L. Iversen, J. Jiang, J. Li, C.F. Spurney, A. Sali, A.D. Guerron, K. Nagaraju, T. Doran, P. Lu, X. Xiao, Q.L. Lu, Effective rescue of dystrophin improves cardiac function in dystrophin-deficient mice by a modified morpholino oligomer, Proc. Natl. Acad. Sci. U. S. A. 105 (2008) 14814–14819.
[52] H.G. Lidov, L.M. Kunkel, Dystrophin and Dp140 in the adult rodent kidney, Lab. Investig. 78 (1998) 1543–1551.
[53] K. Ito, S. Kimura, S. Ozasa, M. Matsukura, M. Ikezawa, K. Yoshioka, H. Ueno, M. Suzuki, K. Araki, K. Yamamura, T. Miwa, G. Dickson, G.D. Thomas, T. Miike, Smooth muscle-specific dystrophin expression improves aberrant vasoregulation in mdx mice, Hum. Mol. Genet. 15 (2006) 2266–2275.
[54] T. Haenggi, J.M. Fritschy, Role of dystrophin and utrophin for assembly and function of the dystrophin glycoprotein complex in non-muscle tissue, Cell. Mol. Life Sci. 63 (2006) 1614–1631.
[55] Y.M. Kobayashi, E.P. Rader, R.W. Crawford, K.P. Campbell, Endpoint measures in the mdx mouse relevant for muscular dystrophy pre-clinical studies, Neuromuscul. Disord. 22 (2012) 34–42.
[56] E.M. Bucholz, R.P. Whitlock, M. Zappitelli, P. Devarajan, J. Eikelboom, A.X. Garg, H.T. Philbrook, P.J. Devereaux, C.D. Krawczeski, P. Kavsak, C. Shortt, C.R. Parikh, Cardiac biomarkers and acute kidney injury after cardiac surgery, Pediatrics 135 (2015) e945–e956.
[57] A. Shirakabe, N. Hata, N. Kobayashi, H. Okazaki, T. Shinada, K. Tomita, M. Yamamoto, M. Tsurumi, M. Matsushita, Y. Yamamoto, S. Yokoyama, K. Asai, W. Shimizu, Serum heart-type fatty acid-binding protein level can be used to detect acute kidney injury on admission and predict an adverse outcome in patients with acute heart failure, Circ. J. 79 (2014) 119–128.
[58] A.K. Erenler, T. Yardan, L. Duran, A. Baydin, Usefulness of heart-type fatty acid binding protein in the emergency department, J. Pak. Med. Assoc. 63 (2013) 1176–1181.
[59] M. Kokot, G. Biolik, D. Ziaja, T. Fojt, L. Kedzierski, K. Antoniak, M. Janowska, K. Pawlicki, K. Ziaja, J. Dulawa, Assessment of subclinical acute kidney injury after abdominal aortic aneurysm surgery using novel markers: L-FABP and H-FABP, Nefrologia 34 (2014) 628–636.
[60] W. Zhou, Q. Guan, C.C. Kwan, H. Chen, M.E. Gleave, C.Y. Nguan, C. Du, Loss of clusterin expression worsens renal ischemia-reperfusion injury, Am. J. Physiol. Ren. Physiol. 298 (2010) F568–F578.
[61] C.Y. Nguan, Q. Guan, M.E. Gleave, C. Du, Promotion of cell proliferation by clusterin in the renal tissue repair phase after ischemia-reperfusion injury, Am. J. Physiol. Ren. Physiol. 306 (2014) F724–F733.
[62] S. Li, Q. Guan, Z. Chen, M.E. Gleave, C.Y. Nguan, C. Du, Reduction of cold ischemia-reperfusion injury by graft-expressing clusterin in heart transplantation, J. Heart Lung Transplant. 30 (2011) 819–826.
[63] K. Vlasakova, Z. Erdos, S.P. Troth, K. McNulty, V. Chapeau-Campredon, N. Mokrzycki, N. Muniappa, Y.Z. Gu, D. Holder, W.J. Bailey, F.D. Sistare, W.E. Glaab, Evaluation of the relative performance of 12 urinary biomarkers for renal safety across 22 rat sensitivity and specificity studies, Toxicol. Sci. 138 (2014) 3–20.
[64] Z.H. Endre, J.W. Pickering, R.J. Walker, P. Devarajan, C.L. Edelstein, J.V. Bonventre, C.M. Frampton, M.R. Bennett, Q. Ma, V.S. Sabbisetti, V.S. Vaidya, A.M. Walcher, G.M. Shaw, S.J. Henderson, M. Nejat, J.B. Schollum, P.M. George, Improved performance of urinary biomarkers of acute kidney injury in the critically ill by stratification for injury duration and baseline renal function, Kidney Int. 79 (2011) 1119–1130.
[65] M. Nejat, J.W. Pickering, P. Devarajan, J.V. Bonventre, C.L. Edelstein, R.J. Walker, Z.H. Endre, Some biomarkers of acute kidney injury are increased in pre-renal acute injury, Kidney Int. 81 (2012) 1254–1262.
[66] A.M. Ralib, J.W. Pickering, G.M. Shaw, P. Devarajan, C.L. Edelstein, J.V. Bonventre, Z.H. Endre, Test characteristics of urinary biomarkers depend on quantitation method in acute kidney injury, J. Am. Soc. Nephrol. 23 (2012) 322–333.
[67] Z. Ghlissi, A. Hakim, H. Mnif, F.M. Ayadi, K. Zeghal, T. Rebai, Z. Sahnoun, Evaluation of colistin nephrotoxicity administered at different doses in the rat model, Ren. Fail. 35 (2013) 1130–1135.
[68] J.A. Gordon, V.H.2nd Gattone, A.C. Schoolwerth, gamma-Glutamyl transpeptidase excretion in cisplatin-induced acute renal failure, Am. J. Kidney Dis. 8 (1986) 18–25.
[69] R.D. Wainford, R.J. Weaver, K.N. Stewart, P. Brown, G.M. Hawksworth, Cisplatin nephrotoxicity is mediated by gamma glutamyltranspeptidase, not via a C-S lyase governed biotransformation pathway, Toxicology 249 (2008) 184–193.